Ceramics-Silikáty 62 (1), 50-58 (2018)
www.ceramics-silikaty.cz doi: 10.13168/cs.2017.0044

EFFECTS OF NiO LOADING AND PRE-CALCINATION TEMPERATURE ON NiO-SDCC COMPOSITE ANODE POWDER FOR LOW-TEMPERATURE SOLID OXIDE FUEL CELLS

N. K. HOA*, #H. A. RAHMAN*, M. R. SOMALU**

*Faculty of Mechanical and Manufacturing Engineering, Universiti Tun Hussein Onn Malaysia, 86400 Batu Pahat, Johor, Malaysia
**Fuel Cell Institute, Universiti Kebangsaan Malaysia, 43600 UKM Bangi, Selangor, Malaysia

#E-mail: hamimah@uthm.edu.my

Submitted July 18, 2017; accepted September 19, 2017

Keywords: Nickel oxide (NiO), Samarium-doped ceria carbonate (SDCC), Calcination, Thermal behaviour, Solid oxide fuel cell

The microstructural and thermal characteristics of NiO-samarium-doped ceria carbonate (NiO–DCC) composite powders have been explored in terms of NiO loading and pre-calcination temperature. NiO–SDCC composite powders were intimately mixed via fast ball-milling using different NiO loadings (50 - 70 wt. %) and subjected to various pre-calcination temperatures (600 - 800°C). Subsequently, the pre-calcined powders were then used to fabricate composite pellets using a uniaxial press and sintered at a low temperature of 600°C. The crystalline phase, carbonate bonding, microstructure and thermal behaviour of the composite anode powders were investigated. The microstructure, porosity, and hardness of sintered composite pellets were also evaluated. All samples maintained their chemical compatibility and carbonate bonding after various processes. The findings indicated that the pre-calcination factor was more important than NiO loading in terms of powder and pellet morphologies as well as the thermal expansion behaviour. Moreover, the composite pellets prepared with composite powders pre-calcined at increasing temperatures exhibited an increase in porosity, but within an acceptable range (30 - 40 %). Overall, composite pellets fabricated with 50 wt. % NiO exhibited the optimum hardness values of 21 - 31 HV and the lowest thermal expansion of 12.2 - 12.7 × 10^{-6} K^{-1}.

INTRODUCTION

In the past decade, continuous efforts have focused on the development of intermediate-to-low-temperature solid oxide fuel cells (IT-LT-SOFCs) operating in the range of 400 - 800°C. The reduction of operating temperature not only lowers the operational cost but also extends the cell stability and durability for effective commercialisation of SOFCs. Unfortunately, a lower operating temperature (< 600°C) deteriorates the electrochemical performance due to large ohmic and anode polarisation resistance [1, 2]. High-performance composite anodes are urgently needed to accelerate the development of IT-LT-SOFCs. Practical strategies that have been adopted to maintain high ionic conductivity and low polarisation resistance include replacing yttria-stabilised zirconia (YSZ) with ceria-based electrolytes as well as optimising the anode microstructures to suppress the polarisation resistance at reduced temperature (400 - 600°C) [3-5].

The anodic electrochemical performance is strongly dependent on the two factors that ultimately define the anode microstructure: (1) composite anode composition and (2) powder processing. According to percolation theory, at least 30 vol. % of the Ni metal loading is required to give sufficient porosity (20 - 40 %) for gas transport and excellent electrical conductivity (>100 S·cm^{-1}) [6]. Moreover, a suitable powder composition is important for achieving minimal thermal mismatch with the electrolyte to prevent spallation at the anode–electrolyte interface upon fabrication and operation [7, 8]. Additionally, powder processing such as pre-calcination has been found to significantly influence the powder morphological properties such as particle size and surface area. Nano-submicron-sized particles with large surface areas extend the triple phase boundary (TPB) and provide homogenous anode microstructure, which ultimately improving the electrochemical performance. Consequently, several researchers have focused exclusively on these two aforementioned critical factors with the aim to develop high performance anode such as Ni-SDC (samarium-doped ceria) and Ni-GDC (gadolinium-doped ceria) composite anodes, resulting in suitable anode microstructural properties and thermal matching, which are equally important considerations for the development of composite anodes [9–11].

Currently, composite anode materials with ceria-based electrolytes such as Ni-SDC and Ni-GDC only exhibit promising cell performance that is limited to intermediate-temperature applications (600 - 800°C) [8, 12-14]. Doped ceria electrolytes have been shown to cause performance degradation due to chemical and mechanical instabilities in the LT region [15]. The addition of binary lithium and sodium carbonate to SDC, forming SDC carbonate (SDCC) electrolyte resolved these issues and with conferred distinctive performance at temperatures below 600°C [16, 17]. NiO-samarium-doped ceria carbonate (NiO-SDCC) has been explored for its excellent compatibility as LT anode with other SOFC components [18–20]. Jarot et al. [21] reported on the feasibility of NiO-SDCC as composite anode with the NiO loading of 60 wt. % and subsequently pre-calcined at 680°C. The pre-calcination step was conducted to allow the carbonate to melt and coat the composite powder. The research revealed a uniform pellet microstructure and satisfactory porosity of 20 - 40 % for anode supported cell application. However, less attention has been devoted to the selection of proper NiO loading and pre-calcination temperature for NiO-SDCC composite powders, which may act as guidance for the development of LT-SOFCs.

In this study, NiO loading and pre-calcination temperatures were systematically varied to explore the microstructural and thermal behaviour of NiO–SDCC composite powders. The characteristic of sintered composite pellets were also evaluated. A fast ball-milling technique was employed to obtain intimately mixed NiO-SDCC composite powders with the NiO loading of 50 - 70 wt. % and pre-calcination from 600 - 800°C was applied. Next, the pre-calcined powders were uniaxially pressed and sintered at 600°C. The crystalline structure, morphology, particle size, surface area, porosity, thermal behaviour, and hardness are reported in this study.

EXPERIMENTAL

Materials and sample preparation

SDC powder (Kceracell, Korea) and $(Li_{0.67}Na_{0.33})CO_3$ (Sigma Aldrich, USA) at the weight ratio of 4:1 were ball-milled in ethanol for 24 h, oven dried, and subsequently calcined at 680°C at a rate of 5°C·min^{-1} for 1 h in air to acquire SDCC electrolyte [18, 21]. The NiO powder (Kceracell, Korea) and aforementioned SDCC powder were ball-milled at different weight ratios (50 - 70 wt. %) for 2 h at 550 rpm and subsequently oven dried to obtain NiO-SDCC composite powder. Hereafter, the samples are denoted as NC55, NC64 and NC73 ("55" denotes 50 wt. % NiO and 50 % wt. % SDCC, and so on), respectively. The as-prepared composite powders were assigned for pre-calcination at 600, 650, 700, 750, and 800°C. The pre-calcination process was controlled at a rate of 5°C·min^{-1} for 1 h in air to allow the carbonate to melt and coat the composite powders. Afterwards, the pre-calcined powders were pressed into pellets (13 mm in diameter) and rods (6 mm in diameter) and sintered at 600°C in air at a rate of 2°C·min^{-1} for 1 h.

Characterisation

An X-ray diffractometer (XRD, D8 Advance-Bruker, Germany), with Cu-Kα radiation (wavelength: 1.5406 Å) was used to determine the crystalline phases. The diffraction patterns were acquired with a scanning interval of 0.02° within the 2θ range of 10 - 80°. Fourier transform infrared spectroscopy (FTIR, Spectrum 100, PerkinElmer, USA) analysis was performed based on the attenuated total reflectance (ATR) within the range of 4000 - 550 cm^{-1}. Thermogravimetric (TG) analysis was carried out (Thermobalance, Linseis, Germany) from 30 to 900°C. The thermal expansion coefficient (TEC) was obtained via a dilatometer (L75H-Linseis, Germany) from 30 to 600°C using fabricated rod samples and alumina as a standard reference sample. The specific surface area was measured using nitrogen adsorption based on the standard Brunauer-Emmett-Teller (BET) model (ASAP 2020, USA). The powder and pellet cross-sectional morphologies were observed using field emission scanning electron microscopy (FESEM, JSM 6700F, Jeol, Japan). Scanning electron microscopy (SEM) attached with energy dispersive X-ray spectroscopy (EDS, JSM 6380LA, Jeol, Japan) was used to obtain the elemental mapping of the composite anode powder. The samples were gold coated (JFC-1600, Jeol, Japan) to improve surface conductivity prior observation. Image J software (Version 4.18) was used to determine the average particle size of the composite powders. The porosity of the anode pellets was measured in ethanol based on the standard Archimedes principle using a density kit (Mettler Toledo, USA). The Vickers indentation hardness measurements was performed on sintered pellets using a HMV-2 microhardness tester (Shimadzu, Japan) with an applied load of 200 g for 15 s [22].

RESULTS AND DISCUSSION

Characteristics of composite powders

The X-ray pattern of NiO-SDCC composite powders (NC55-NC73) pre-calcined at 800°C is shown in Figure 1. The diffractogram was indexed well with the cubic structure of NiO (space group of Fm-3m, JCPDS:47-1049) and SDCC (space group of Fm-3m, JCPDS:75-0158) respectively. For comparison, the XRD patterns of pure NiO and SDCC are displayed in the same diagram. Meanwhile, the diffractograms of NC64 composite pellets prepared from varied pre-calcination temperatures shown in Figure 2 also demonstrated similar results. Good chemical compatibility was observed since no secondary constituent was detected after various

processes. The lattice parameters of NiO (4.171 - 4.180 Å) and SDCC (5.421-5.425 Å) were also close to the standard lattice parameters of NiO (4.177 Å) and SDCC (5.423 Å), respectively. The carbonate was undetected in the XRD pattern due to its presence as amorphous coating around the powders after the pre-calcination process, which is coherent with other studies [19, 21]. The amorphous carbonate layer is clearly evidenced in the TEM image, as shown in Figure 3, which is essential to retain the fast multi-ionic conductions (H^+ and O^{2-}) and to provide good cell performance typically in the LT region [23].

The existence of the carbonate layer on composite powders is further clarified using FTIR analysis. The FTIR spectra (Figure 4) obtained for NC55 composite powders shows the presence of transmission signals recorded around 1463 - 1431 cm^{-1} (intense and broad peaks) and 861 - 862 cm^{-1} (sharp peak) [24], corresponding to stretching and bending vibrations of the carbonate (CO_3^{2-}) anion. A similar observation was obtained for the rest of samples in this study. The signal intensity of the infrared peaks of the carbonate also gradually decreased with the increase of calcination temperature, with the lowest carbonate intensity being found at the highest pre-calcination temperature of 800°C (Figure 4). This observation may be attributed to the start of carbonate decomposition, which takes place beyond the melting point of carbonate, as will be further discussed later.

The FESEM images of NC73 pre-calcined at various temperatures are shown in Figure 5. Nano-submicron-sized and uniform particles were observed in all samples. For qualitative comparison, the particle size increased with increases in pre-calcination temperature. Similarly, composite powders prepared with increasing NiO loading (NC55–NC73) showed a slight increment in particle size, mainly due to NiO coarsening, as observed in Figure 6 [7]. Meanwhile, the correlation between measured average particle size and BET surface area is illustrated in Figure 7. The composite powders of NC55, NC64, and NC73 have average particle sizes of around 83.5 - 126.2, 83.8 - 128.7, and 87.0 - 148.5 nm, corresponding to surface areas of 2.0 - 7.0, 3.6 - 6.0,

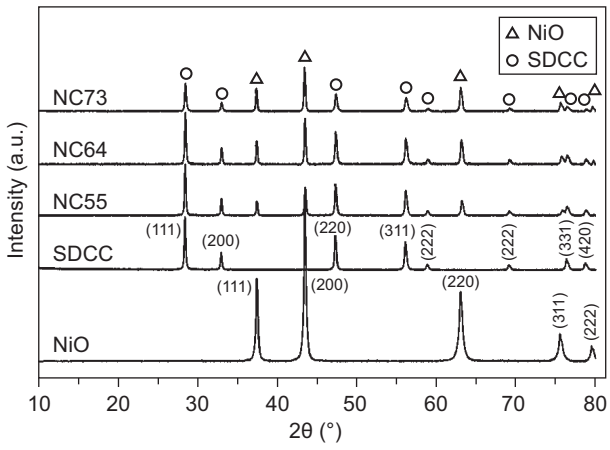

Figure 1. X-ray pattern of NC55, NC64 and NC73 composite powders pre-calcined at 800°C 95 × 127 mm.

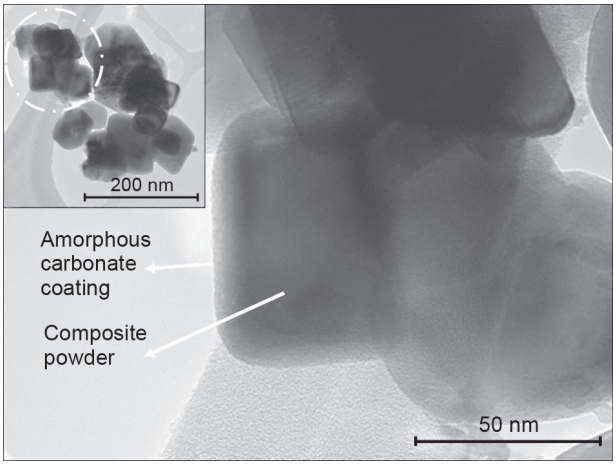

Figure 3. TEM image of NC55 with amorphous carbonate coating around NiO-SDCC composite powder: 121 × 155 mm.

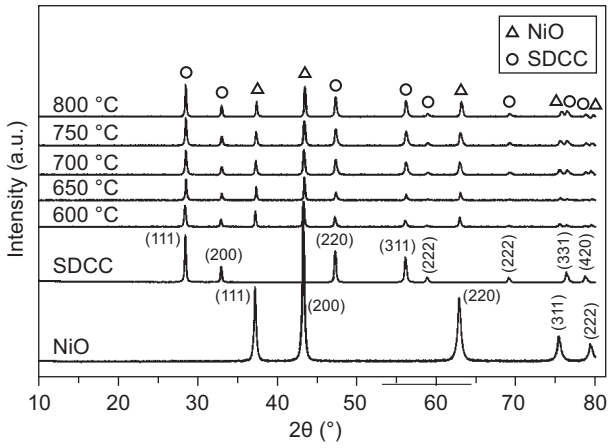

Figure 2. X-ray pattern of NC64 sintered composite pellets fabricated from various pre-calcined powders: 95 × 127 mm.

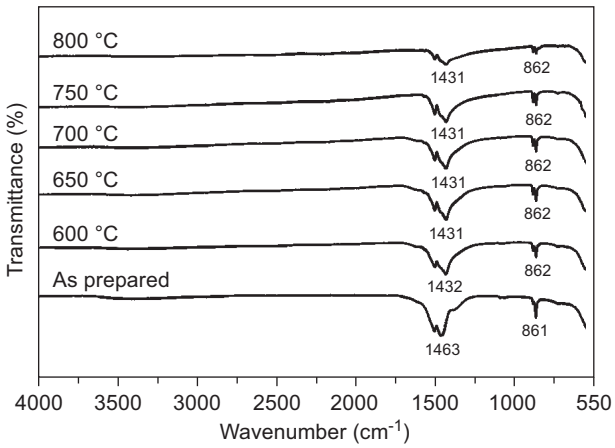

Figure 4. FTIR spectra of NC55 composite powders FTIR spectra of NC55 composite powders: 111 × 145 mm.

and 3.6 - 8.4 $m^2 \cdot g^{-1}$, respectively. This shows that the influence of pre-calcination temperature is dominant, as it contributed almost 71 % of the increment of average particle size, whereas the NiO loading contributed only up to 18 %. The obtained surface area is also comparable to that found in previous studies; that it is essential for gas adsorption–diffusion and good electrochemical performance. For example, Yin et al. [25], Sato et al. [26] and Somalu et al. [6] reported surface areas of 9, 7, and 4 - 8 $m^2 \cdot g^{-1}$ for NiO–SDC, NiO–YSZ, and NiO–ScSz composite anode powders, respectively. The homogeneity of the NiO-SDCC powder was also verified using the EDS mapping technique. Figure 8 represents the elemental mapping and EDS spectrum of NC55 pre-calcined at 600°C, clearly showing the well elemental distribution of sodium (Na), nickel (Ni), cerium (Ce), and samarium (S·m) within the mapped region. Powder characteristics with nano-submicron size (< 1 μm) and good elemental distribution are essential to provide well-connected TPBs, which behave as reaction sites that enhance the electrochemical performance [9].

The TG curves of NC55, NC64, and NC73 composite powders acquired from 30 to 900°C are shown in Figure 9. The total weight loss of the composite powders decreased with increasing amount of SDCC electrolyte. Weight loss occurring in the temperature ranges from 30 - 100°C and 100 - 400°C was presumed to be mainly due to evaporation and dehydroxylation of adsorbed water. A slight mass loss (~ 1 - 2 %) was

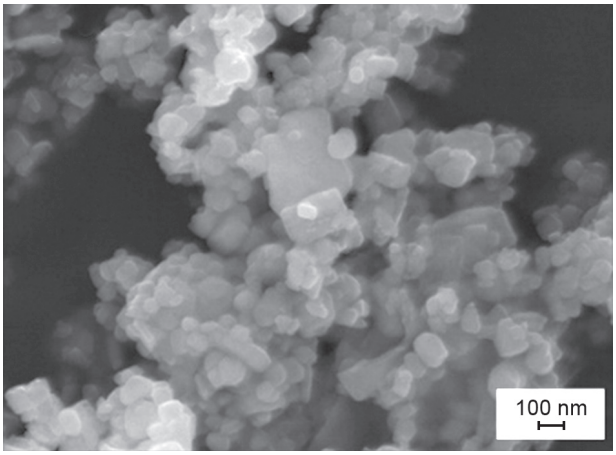

a) 600°C

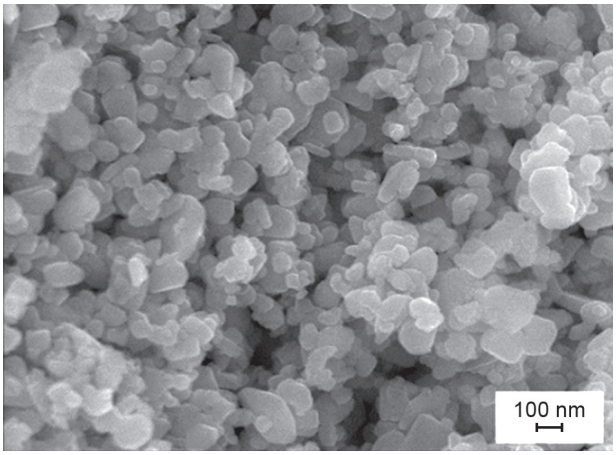

b) 650°C

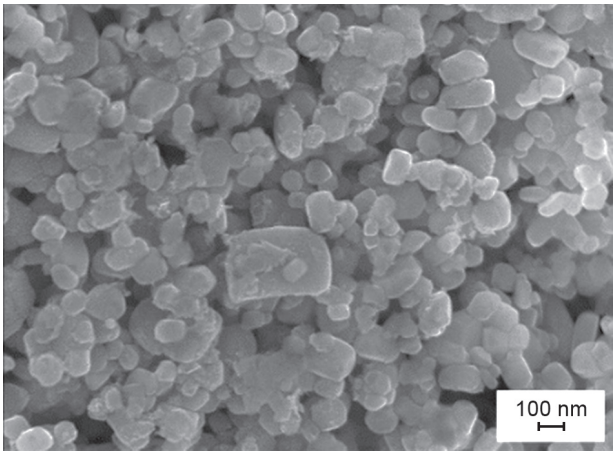

d) 750°C

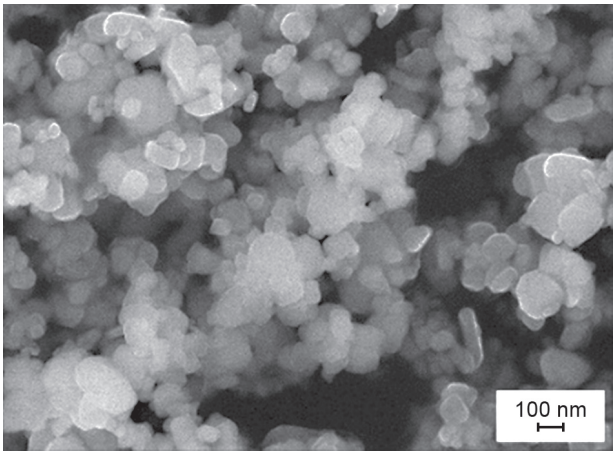

c) 700°C

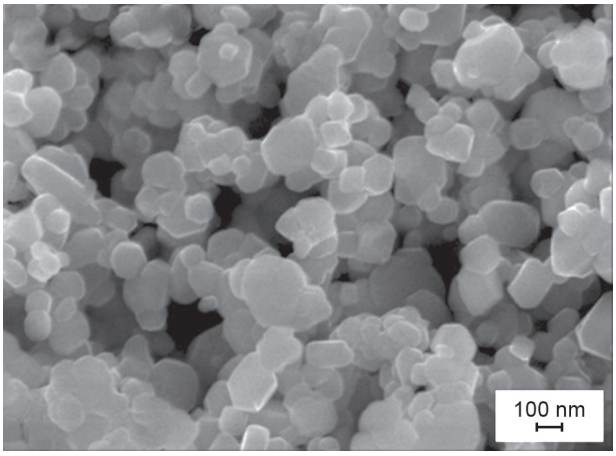

e) 800°C

Figure 5. FESEM images of NC73 powders pre-calcined a) 600°C, b) 650°C, c) 700°C, d) 750°C, and e) 800°C: 168 × 149 mm.

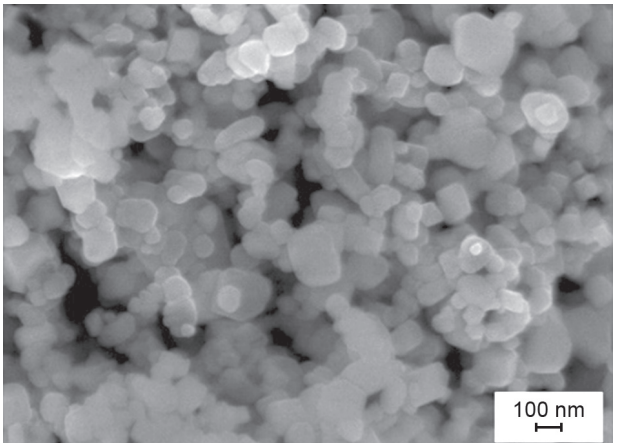

a) NC55

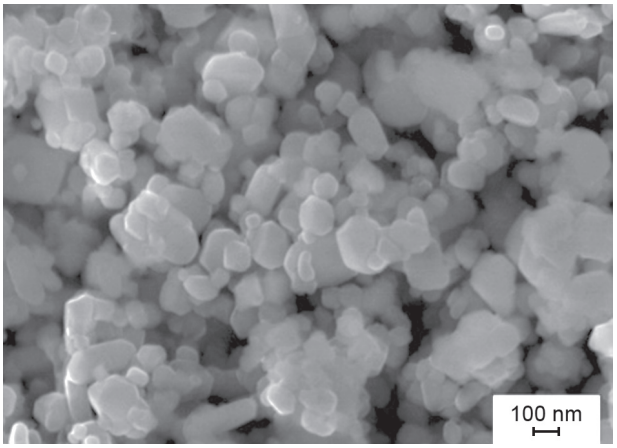

b) NC64

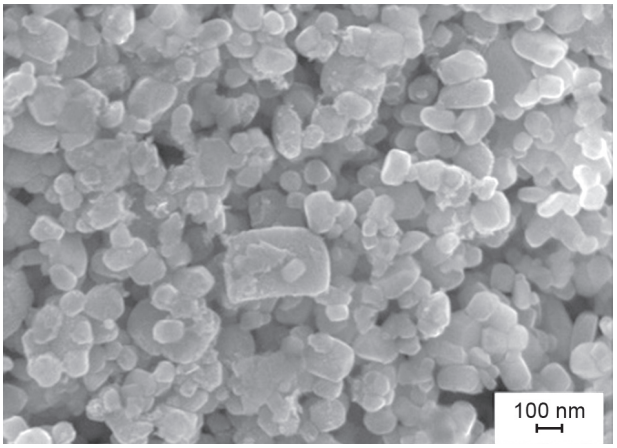

c) NC73

Figure 6. FESEM images of a) NC55, b) NC64 and c) NC73 pre-calcined at 750°C: 112 × 149 mm.

observed in the range of 400 - 600°C in all composite powders due to melting of the carbonate, indicating that no serious volatilization or decomposition of carbonates occurred in any of these NiO-SDCCs. Meanwhile, the melting process is necessary to ensure carbonate coating on the composite particles, which is coherent with other studies [23, 27, 28]. All NiO-SDCCs also demonstrated less pronounced total mass losses (< 7 %) from 30 to 900°C. Furthermore, the presence of carbonate coating on the composite powders is demonstrated by the TEM image (Figure 4) and FTIR analysis (Figure 5) earlier. The TG information also clarifies that the selection of pre-calcination and sintering remains relevant for SOFC operation within the LT region (< 600°C)[17].

Table 1 shows the average TEC values obtained in the temperature range of 30 - 600°C. Minimising thermal mismatch with the electrolyte is the key to good thermo-mechanical compatibility during cell fabrication and operation. At the same pre-calcination temperature, the TEC trend increases gradually with NiO loading due to the slightly larger TEC value of NiO (14.14×10^{-6} K^{-1}) as compared to SDCC (12.17×10^{-6} K^{-1}). On the other hand, the TEC behaviour also increases with the increase of pre-calcination temperature. A plausible explanation for this phenomenon is that the slight increase in particle size is induced by a corresponding increase of the pre-calcination temperature at a given NiO loading. This was confirmed by FESEM analysis earlier. Particles of smaller size have a tendency to attain lower TEC values compared to larger particles [5]. For the anode

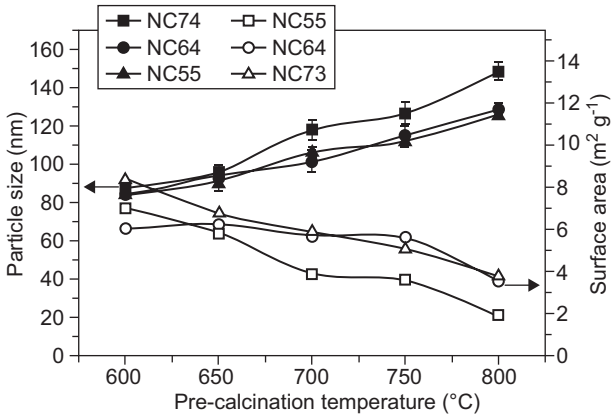

Figure 7. Average particle size and surface area of NiO–SDCC composite powders with respect to NiO loading and pre-calcination temperatures: 91 × 140 mm.

Table 1. Average TEC for NiO–SDCCs obtained from 30 to 600°C.

Pre-calcination temperature (°C)	Thermal expansion coefficient, TEC ($\times 10^{-6}$ K^{-1}) (30 - 600°C)				
	NiO	SDCC	NC55	NC64	NC73
600	14.14 ± 0.19	12.17 ± 0.70	12.21 ± 0.55	12.46 ± 0.62	12.81 ± 0.67
650	–	–	12.23 ± 0.17	12.51 ± 0.62	13.00 ± 0.52
700	–	–	12.22 ± 0.46	12.59 ± 0.49	13.11 ± 0.16
750	–	–	12.53 ± 0.56	12.61 ± 0.17	13.11 ± 0.67
800	–	–	12.70 ± 0.65	12.84 ± 0.36	13.13 ± 0.30

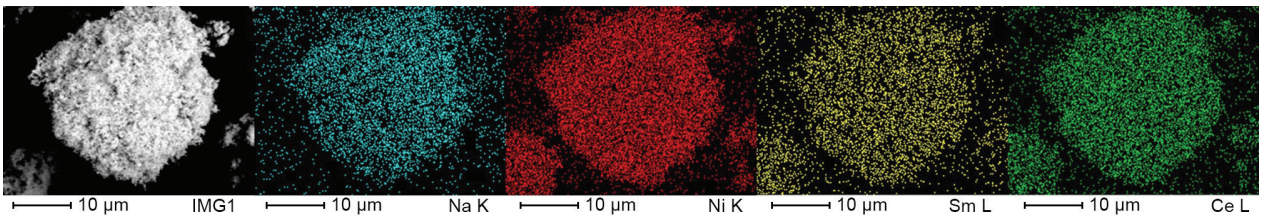

a)

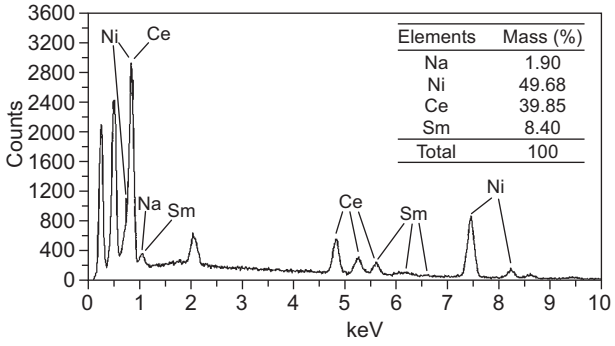

b)

Figure 8. EDS spectrum and corresponding elemental mapping of NC64 composite powder pre-calcined at 600°C: 150 × 149 mm.

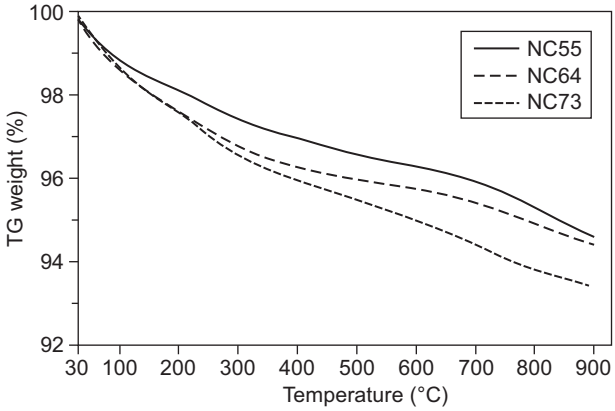

Figure 9. TG curves of NiO-SDCC: 120 × 159 mm.

component, the permissible TEC difference lies within 15 - 20 % if good thermo-mechanical compatibility is to be attained [8]. Based on this requirement, the TEC difference for all samples was within 0.3 - 7.9 %, which suggests excellent thermal compatibility with the SDCC electrolyte.

Microstructure of sintered composite pellets

According to Fan et al.[29], the presence of carbonates also acts as a sintering aid for SOFC electrodes, which is beneficial for a lower sintering temperature of about 600°C. Such an approach promotes better control of porosity without the usage of pore forming agent as compared to the conventional sintering step (> 800°C). In this study, the pre-calcined NiO-SDCC composite powers of various temperatures (600 - 800°C) were uniaxially pressed and sintered at 600°C to evaluate the microstructure of sintered composite pellets

The increment of NiO loading (NC55-NC73) increases the porosity from 31 - 37 % at a given precalcination temperature as shown in Figure 10. Most researchers reported the same trend of porosity with increasing Ni loading up to 70 vol. %, which can be associated with the uniform microstructural features of the fabricated composite pellets [10, 25]. However, pre-calcination temperature factor has a more pronounced effect than the NiO loading on the porosity of NiO–SDCC. A monotonous increment of porosity can be observed as the pre-calcination temperature increases from 600 to 800°C at a given NiO loading, which could

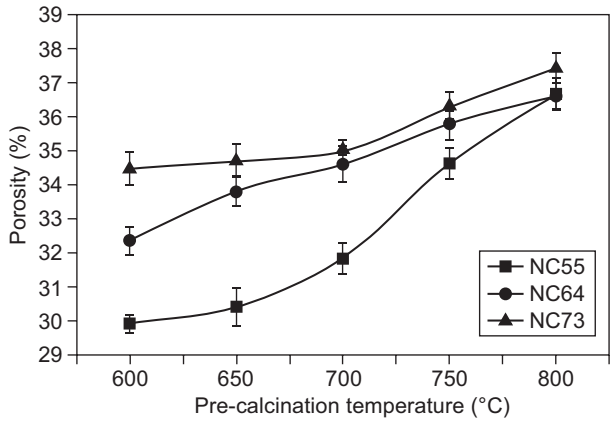

Figure 10. Porosity results of sintered composite pellets: 93 × 147 mm.

be related to the larger particle size induced, as described earlier. According to Herring's law of sintering, smaller particles potentially retain higher densification kinetics compared to larger particles sintered at the same sintering temperature (600°C) [10]. The porosity result is also coherent with the cross-sectional FESEM morphologies shown in Figures 11 and 12. Well-connected grains and uniform porous structure of the pellets became more apparent in powders pre-calcined at increasing temperature as shown in Figure 11. Meanwhile, Figure 12 shows a slight increment of porosity and grain size variation in pellet prepared with different NiO loadings. Furthermore, all composite pellets provide satisfactory porosity of ~30 %, which is essential for gaseous transport and to provide a good anodic reaction in anode-supported cells [6].

Besides the excellent chemical compatibility and adequate porosity level of NiO–SDCC, investigation of its mechanical features such as hardness is important, especially for porous anode-supported cell applications. Figure 13 represents the Vickers hardness results for NiO–SDCC composite pellets. A decrease in Vickers hardness was observed regardless of NiO loading or pre-calcination temperature. This trend is expected due to the increase in porosity and grain size that was discussed earlier, which generally reduces the mechanical strength. NC55 with the NiO loading of 50 wt.% exhibited a higher hardness value (21-31 HV) as compared to NC64 (19-29 HV) and NC73 (18-27 HV). Up to date, there are still limited studies regarding the mechanical properties of composite electrodes with ceria carbonate-based electrolyte. However, the present result is as good as those for other composite pellets sintered at high temperature. For example, Shaikh et al. [30] obtained a hardness value of 30 HV corresponding to a porosity level of 33 % in CuO-SDC composite pellets sintered at 900°C. In general, reduction process in hydrogen atmosphere will lead to an increase in the porosity level due to conversion of NiO to Ni, forming Ni–SDCC cermets [22]. Thus, further investigation of the mechanical strength is necessary for Ni–SDCC cermet to evaluate its potential for application as anode-supported cells.

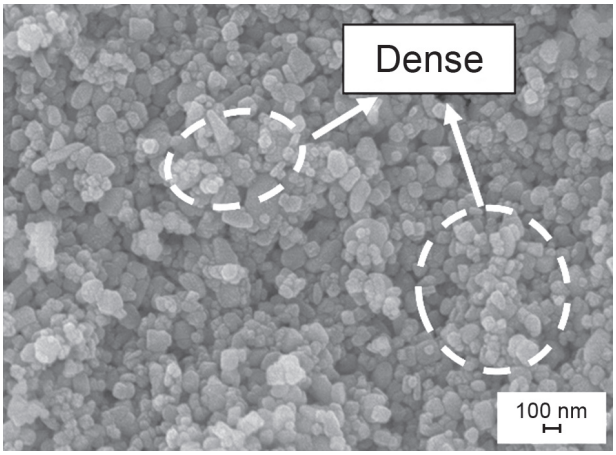

a) 600°C

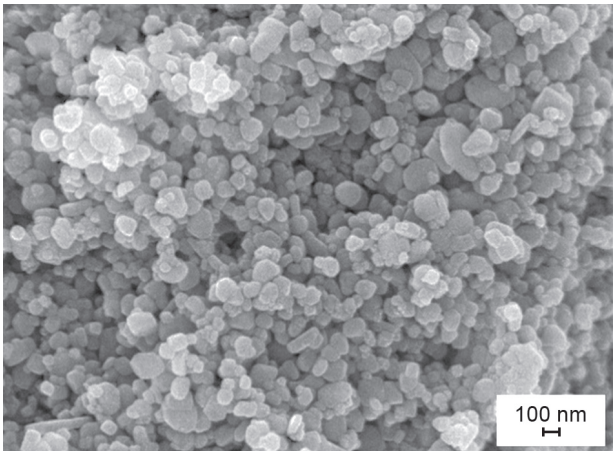

b) 650°C

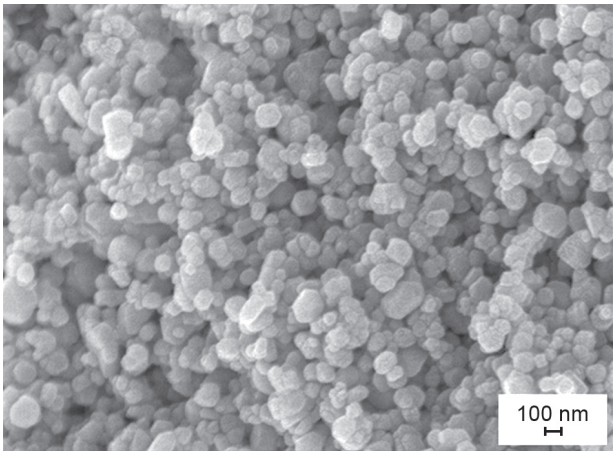

d) 750°C

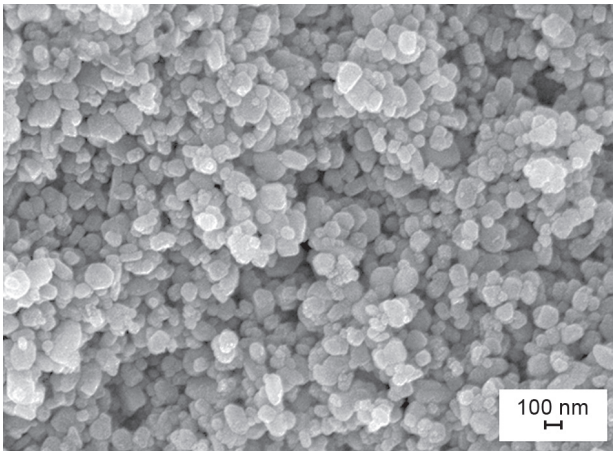

c) 700°C

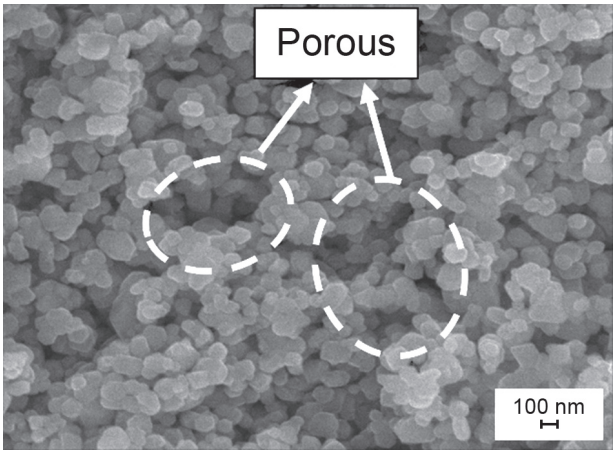

e) 800°C

Figure 11. FESEM micrographs of NC73 sintered composite pellets prepared from powders pre-calcined at a) 600°C, b) 650°C, c) 700°C, (d) 750°C, and e) 800°C: 166 × 125 mm.

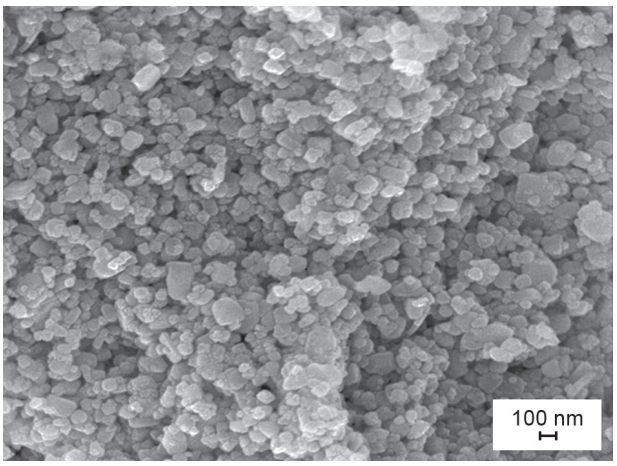

a) NC55

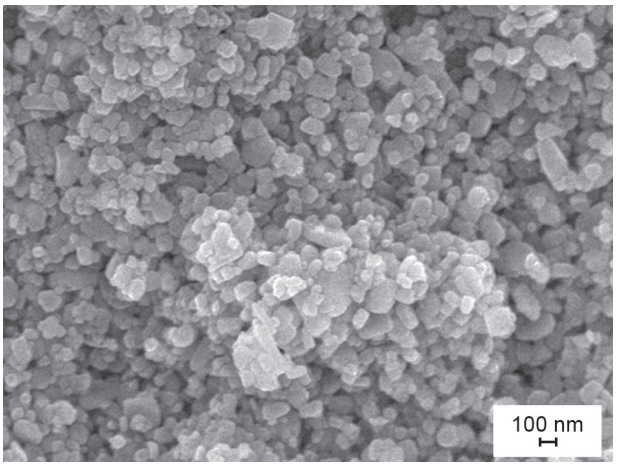

b) NC64

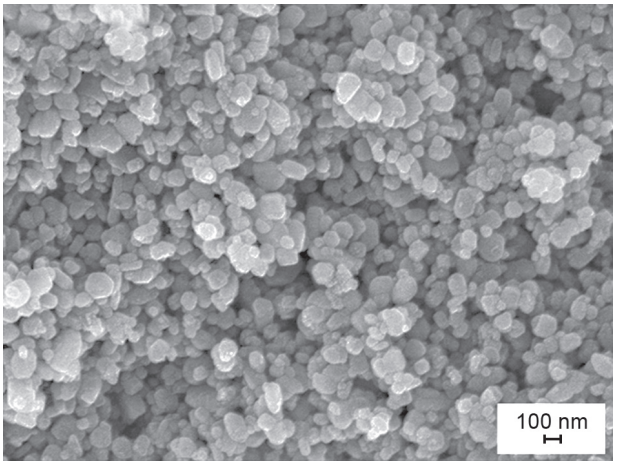

c) NC73

Figure 12. FESEM micrographs of sintered a) NC55, b) NC64 and c) NC73 composite pellets prepared from powder pre-calcined at 700°C: 112 ×149 mm.

CONCLUSION

The microstructure and thermal behaviour of the composite powders have been investigated based on different NiO loadings and calcination temperatures.

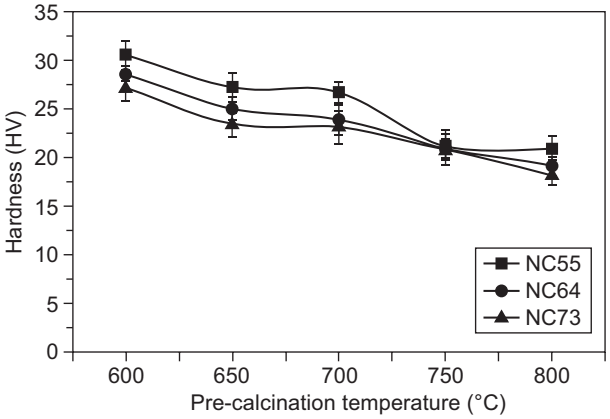

Figure 13. Hardness of sintered composite pellets as a function of pre-calcination temperature: 93 × 135 mm.

The composite powders maintain their crystalline phases after the fast milling, calcination, and sintering processes. The particle size and thermal expansion coefficient of NiO–SDCC were found to be strongly influenced by the changes in calcination temperature compared to NiO loading. Likewise, the microstructure and porosity of the pellets were also found to be more affected by the calcination temperature factor. In brief, all samples in the present study exhibited high potential as anode material for SOFCs due to their: (1) good chemical compatibility, (2) low thermal mismatch, and (3) sufficient porosity level. In particular, NC55 was found to be the more outstanding compared to other NiO loadings, within the pre-calcination range of 600 - 800°C as it had the lowest thermal mismatch and highest hardness value, which are important for anode supported application. To evaluate the potential of NC55, electrical conductivity, electrochemical characterisation, and mechanical studies will be conducted in future with regard to the low temperature region.

Acknowledgements

The authors gratefully acknowledge research funds from Universiti Tun Hussein Onn Malaysia (UTHM) and the Ministry of Higher Education Malaysia under RACE-Vot 1512. The first author also acknowledges the Malaysian Ministry of Education for postgraduate sponsorship under the MyBrain 15 scheme.

REFERENCES

1. Wachsman E., Ishihara T., Kilner J. (2014): Low-temperature solid-oxide fuel cells. *MRS Bulletin, 39*, 773–779. doi:10.1557/mrs.2014.192.
2. Baharuddin N.A., Muchtar A., M.R. Somalu (2016): Influence of sintering temperature on the polarization resistance of $La_{0.6}Sr_{0.4}Co_{0.2}Fe_{0.8}O_{3-\delta}$ – SDC carbonate composite cathode. *Ceramics – Silikaty, 60*, 1–9. doi:10.13168/cs.2016.0017.

3. Mahmud L.S., Muchtar A., Somalu M.R. (2016): Influence of sintering temperature on NiO–SDCC Anode For Low-Temperature Solid Oxide Fuel Cells (LT-SOFCs). *Ceramics – Silikaty, 60,* 317–323. doi:10.13168/cs.2016.0047.
4. Lee K.T., Wachsman E.D. (2014): Role of nanostructures on SOFC performance at reduced temperatures. *MRS Bulletin*, *39*, 783–791. doi:10.1557/mrs.2014.193.
5. Ahmadrezaei M., Ali S.A.M., Muchtar A., Tan C.Y., Somalu M.R. (2014): Thermal expansion behavior of the $Ba_{0.2}Sr_{0.8}Co_{0.8}Fe_{0.2}O_{3-d}$ (BSCF) with $Sm_{0.2}Ce_{0.8}O_{1.9}$. *Ceramics – Silikáty, 58*, 46–49.
6. Somalu M.R., Yufit V., Cumming D., Lorente E., Brandon N.P. (2011): Fabrication and characterization of Ni/ScSZ cermet anodes for IT-SOFCs. *International Journal of Hydrogen Energy,* 36, 5557–5566. doi:10.1016/j.ijhydene.2011.01.151.
7. Shri Prakash B., Senthil Kumar S., Aruna S.T. (2014): Properties and development of Ni/YSZ as an anode material in solid oxide fuel cell: A review. *Renewable and Sustainable Energy Review, 36*, 149–179. doi:10.1016/j.rser.2014.04.043.
8. Chen M., Kim B.H., Xu Q., Ahn B.G., Huang D.P. (2010): Effect of Ni content on the microstructure and electrochemical properties of Ni–SDC anodes for IT-SOFC. *Solid State Ionics, 181*, 1119–1124. doi:10.1016/j.ssi.2010.06.030.
9. Kim Y.M., Baek S.W., Bae J.M., Yoo Y.S. (2011): Effect of calcination temperature on electrochemical properties of cathodes for solid oxide fuel cells. *Solid State Ionics, 192*, 595–598. doi:10.1016/j.ssi.2010.09.014.
10. Chen M., Kim B.H., Xu Q., Ahn B.G. (2009): Preparation and electrochemical properties of Ni–SDC thin films for IT-SOFC anode. *Journal of Membrane Science, 334*, 138–147. doi:10.1016/j.memsci.2009.02.023.
11. Sugihara K., Asamoto M., Itagaki Y., Takemasa T., Yamaguchi S., Sadaoka Y. (2014): A quantitative analysis of influence of Ni particle size of SDC-supported anode on SOFC performance: Effect of particle size of SDC support. *Solid State Ionics, 262*, 433–437. doi:10.1016/j.ssi.2014.02.012.
12. Seyednezhad M., Rajabi A., Muchtar A., Somalu M.R. (2015): Characterization of IT-SOFC non-symmetrical anode sintered through conventional furnace and microwave. *Ceramics International, 41*, 5663–5669. doi:10.1016/j.ceramint.2014.12.151.
13. Gil V., Tartaj J., Moure C. (2009): Chemical and thermomechanical compatibility between Ni – GDC anode and electrolytes based on ceria. *Ceramics International, 35*, 839–846. doi:10.1016/j.ceramint.2008.03.004.
14. Torknik F.S., Keyanpour-Rad M., Maghsoudipour A., Choi G.M. (2014): Effect of microstructure refinement on performance of $Ni/Ce_{0.8}Gd_{0.2}O_{1.9}$ anodes for low temperature solid oxide fuel cell. *Ceramics International, 40*, 1341–1350. doi:10.1016/j.ceramint.2013.07.015.
15. Jing Y., Patakangas J., Lund P.D., Zhu B. (2013): An improved synthesis method of ceria-carbonate based composite electrolytes for low-temperature SOFC fuel cells. *International Journal of Hydrogen Energy, 38*, 16532–16538. doi:10.1016/j.ijhydene.2013.05.136.
16. Chockalingam R., Basu S. (2011): Impedance spectroscopy studies of $Gd–CeO_2–(LiNa)CO_3$ nano composite electrolytes for low temperature SOFC applications. *International Journal of Hydrogen Energy, 36*, 14977–14983. doi:10.1016/j.ijhydene.2011.03.165.
17. Ma Y., Wang X., Raza R., Muhammed M., Zhu B. (2010): Thermal stability study of SDC/Na_2CO_3 nanocomposite electrolyte for low-temperature SOFCs. *International Journal of Hydrogen Energy, 35*, 2580–2585. doi:10.1016/j.ijhydene.2009.03.052.
18. Rahman H.A., Muchtar A., Muhamad N., Abdullah H. (2013): $La_{0.6}Sr_{0.4}Co_{0.2}Fe_{0.8}O_{3-\delta}$–SDC carbonate composite cathodes for low-temperature solid oxide fuel cells. *Materials Chemistry and Physics, 141*, 752–757. doi:10.1016/j.matchemphys.2013.05.071.
19. Di J., Chen M., Wang C., Zheng J., Fan L., Zhu B. (2010): Samarium doped ceria–$(Li/Na)_2CO_3$ composite electrolyte and its electrochemical properties in low temperature solid oxide fuel cell. *Journal of Power Sources, 195*, 4695–4699. doi:10.1016/j.jpowsour.2010.02.066.
20. Fan L., Chen M., Wang C., Zhu B. (2012): Pr_2NiO_4–Ag composite cathode for low temperature solid oxide fuel cells with ceria-carbonate composite electrolyte. *International Journal of Hydrogen Energy, 37*, 19388–19394. doi:10.1016/j.ijhydene.2011.09.124.
21. Jarot R., Muchtar A., Wan Daud W.R., Muhamad N., Majlan E.H. (2011): Porous NiO-SDC Carbonates Composite Anode for LT-SOFC Applications Produced by Pressureless Sintering. *Applied Mechanics and Materials, 52–54*, 488–493. doi:10.4028/www.scientific.net/AMM.52-54.488.
22. Fan X., Case E.D., Yang Q., Nicholas J.D. (2013): Room temperature hardness of gadolinia-doped ceria as a function of porosity. *Journal of Materials Science, 48*, 6977–6985. doi:10.1007/s10853-013-7506-3.
23. Chen M., Zhang H., Fan L., Wang C., Zhu B. (2014): Ceria-carbonate composite for low temperature solid oxide fuel cell: Sintering aid and composite effect. *International Journal of Hydrogen Energy, 39*, 12309–12316. doi:10.1016/j.ijhydene.2014.04.004.
24. Coates J. (2000). Interpretation of Infrared Spectra. A practical approach, in: Meyers R.A. (Ed.): *Encyclopedia of Analytical Chemistry*. John Wiley & Sons, Inc. pp. 10815–10837. doi:10.1002/9780470027318.
25. Yin Y., Zhu W., Xia C., Meng G. (2004): Gel-cast NiO–SDC composites as anodes for solid oxide fuel cells. *Journal of Power Sources, 132*, 36–41. doi:10.1016/j.jpowsour. 2004. 01.017.
26. Sato K., Abe H., Misono T., Murata K., Fukui T., Naito M. (2009): Enhanced electrochemical activity and long-term stability of Ni–YSZ anode derived from NiO–YSZ interdispersed composite particles. *Journal of the European Ceramic Society, 29*, 1119–1124. doi:10.1016/j.jeurceramsoc.2008.07.050.
27. Xie F., Wang C., Mao Z., Zhan Z. (2014): Thermal stability study of $La_{0.9}Sr_{0.1}Ga_{0.8}Mg_{0.2}O_{2.85}$–$(Li/Na)_2CO_3$ composite electrolytes for low-temperature solid oxide fuel cells. *International Journal of Hydrogen Energy. 39*, 14397–14401. doi:10.1016/j.ijhydene.2014.02.094.
28. Ristoiu T., Petrisor T., Gabor M., Rada S., Popa F., Ciontea L. (2012): Electrical properties of ceria/carbonate nanocomposites. *Journal of Alloys and Compounds, 532*, 109–113. doi:10.1016/j.jallcom.2012.03.098.
29. Fan L., He C., Zhu B. (2017): Role of carbonate phase in ceria-carbonate composite for low temperature solid oxide fuel cells: A review. *International Journal of Energy Research*, *41*, 465–481. doi:10.1002/er.3629.
30. Shaikh S.P.S., Somalu M.R., Muchtar A. (2016): Nanostructured Cu-CGO anodes fabricated using a microwave-assisted glycine-nitrate process. *Journal of Physics and Chemistry of Solids, 98*, 91–99. doi:10.1016/j.jpcs.2016.06.016.